Physical properties of polyacrylamide gels probed by AFM and rheology

— Source link ↗

Yara Abidine, Yara Abidine, Valérie M. Laurent, Valérie M. Laurent ...+7 more authors

Institutions: University of Grenoble, Centre national de la recherche scientifique, French Institute of Health and Medical Research, University of Lyon

Topics: Glass transition, Viscoelasticity, Rheology and Rheometer

Related papers:

- Determination of elastic moduli of thin layers of soft material using the atomic force microscope.

- Microrheology of Human Lung Epithelial Cells Measured by Atomic Force Microscopy

- Soft biological materials and their impact on cell function

- Tissue Cells Feel and Respond to the Stiffness of Their Substrate

- Effects of substrate stiffness on cell morphology, cytoskeletal structure, and adhesion

Share this paper: 𝟎 🐦 in ✉

View more about this paper here: https://typeset.io/papers/physical-properties-of-polyacrylamide-gels-probed-by-afm-and-mxfb1lvl8f

Physical properties of polyacrylamide gels probed by AFM and rheology

Yara Abidine, Valérie Laurent, Richard Michel, Alain Duperray, Liviu Iulian Palade, Claude Verdier

HAL Id: hal-00840468

https://hal.archives-ouvertes.fr/hal-00840468v4

Submitted on 27 Jan 2015

Physical properties of polyacrylamide gels probed by AFM and rheology

Yara Abidine[1,2], Valérie M. Laurent[1,2], Richard Michel[1,2], Alain Duperray[3,4]
Liviu Iulian Palade[5] (a) and Claude Verdier[1,2] (b)

[1] *Univ. Grenoble Alpes, LIPHY, F-38000 Grenoble, France*
[2] *CNRS, LIPHY, F-38000 Grenoble, France*
[3] *INSERM, IAB, F-38000 Grenoble, France*
[4] *Univ. Grenoble Alpes, IAB, F-38000 Grenoble, France*
[5] *Université Lyon, CNRS, Institut Camille Jordan, UMR 5208, INSA-Lyon, Pôle de Mathématiques, F-69621 Villeurbanne, France*

Abstract. - Polymer gels have been shown to behave as viscoelastic materials but only a small amount of data is usually provided in the glass transition. In this paper, the dynamic moduli G' and G'' of polyacrylamide hydrogels are investigated using both an AFM in contact force modulation mode and a classical rheometer. The validity is shown by matching of the two techniques. Measurements are carried out on gels of increasing polymer concentration in a wide frequency range. A model based on fractional derivatives is successfully used, covering the whole frequency range. G_N^0, the plateau modulus, as well as several other parameters are obtained at low frequencies. The model also predicts the slope a of both moduli in the glass transition, and a transition frequency f_T is introduced to separate the gel–like behavior with the glassy state. Its variation with polymer content c gives a dependence $f_T \sim c^{1.6}$, in good agreement with previous theories. Therefore the AFM data provides new information on the physics of polymer gels.

Introduction. – Polymers exhibit interesting rheological behavior for they can successively behave as liquids, elastic materials showing a rubbery plateau, then undergo a glass transition before reaching the solid domain [1]. These processes are temperature-dependent. Because of this broad range of properties, polymers are widely used in industrial applications, as well as biological processes. However, it is often difficult to characterize their material properties, as the range of relevant frequencies covers several decades [2,3]. Techniques such as classical rheometry, diffusing-wave spectroscopy (DWS) [4], dynamic light scattering [5] or ultrasonic experiments have been used to describe the complex behavior of polymers each in its own range of frequencies [6,7]. In particular, an important way to extend the linear viscoelastic behavior (LVE) is to use the time–temperature superposition principle, wherein results obtained at various temperatures are shifted onto a reference temperature master curve [3]. These observations have motivated quite a lot of theoretical studies. Different models providing relaxation spectra have been proposed, ranging from multiple Maxwell models to continuous relaxation spectra [2], involving both liquid and glassy modes. The concept of soft glassy rheology [8,9] appeared recently and provides another alternative suited for many systems. Indeed it is based on the idea that sub–elements in the microstructure are linked via weak interactions, in a disordered metastable state. Based on this concept, many complex fluids can be described thanks to this model, in particular packed colloidal suspensions, the cell cytoskeleton [10] as well as foams or slurries.

Due to their cross-linked network, polymer gels share similar properties [8] with polymers. They can be characterized using microrheology techniques [11,12], as applied in particular for actin networks [13,14]. The behavior of

---

(a)E-Mail: Liviu-Iulian.Palade@insa-lyon.fr
(b)E-Mail: Claude.Verdier@ujf-grenoble.fr

classical gels is in fact similar in the glass transition domain, but no modelling attempt has been made so far to characterize the entire frequency domain covered by recent instruments. Therefore, it is worthy to characterize various polymeric gels in a wide range of frequencies, and develop a model for the whole range. This is the main purpose of the work presented here. An AFM–based microrheology method [15–18] will be designed to investigate a wider range of frequencies, in combination with classical rheometry. This dynamic AFM technique, used to characterize [19] and probe the mechanical properties locally [16], was developed and validated up to 10 Hz for polymers [15]. Here, we will extend it up to 500 Hz by checking the overlap of the AFM and rheology data. We will choose to characterize polyacrylamide hydrogels due to their widely used mechanical properties [20, 21], in particular in biology. These gels exhibit viscoelastic properties [21], depending on concentration or cross–linking density.

A theoretical model based on a continuous relaxation spectrum modified using fractional derivatives for the higher frequencies [3] will be used to describe the whole rheology spectrum. In the classical rheology domain [0.001 Hz − 2 Hz], information on the plateau modulus G_N^0 [22] will show an increase with a power dependence with acrylamide concentration. Other model parameters will be also discussed. Further data in the high frequency range [1 Hz − 500 Hz] will allow to investigate the glass transition regime (slope a of dynamic moduli) using AFM–microrheology. In particular, a new transition time λ_T between the gel–like region and the glass regime will be introduced and compared to previous theories [23, 24].

Experiments and modelling. –

AFM and rheology measurements. Polyacrylamide gels were synthesized by mixing acrylamide (30% w/w) at four different weight concentrations (5 − 7.5 − 10 − 15%), and N,N–methylene–bisacrylamide 1% w/w at a fixed concentration 0.03% in deionized water. This means that hydrogels were slightly crosslinked. Polymerization was then initiated by incorporating N,N,N,N-tetramethylethylenediamine (TEMED, Sigma) and ammonium persulfate 10% solution (APS), as described earlier [20]. Gels of thickness 70 μm were prepared on a pre–treated glass Petri dish for a better adhesion [20]. Gels were always kept in humid conditions, so that they were swollen and in equilibrium. The Petri dish containing the gel was set onto the AFM (JPK Instruments, Berlin) equipped with an inverted microscope (Zeiss, model D1, Berlin). The AFM chips (Bruker, MLCT, pyramid shape) had 4 sharp sides with an average tip half–angle $\theta = 20^o$. The radius of curvature at the tip was around 20 nm. Stiffness constants used were ~ 0.01 N/m when mounted onto the AFM glass block and were calibrated using the thermal fluctuations method. Then an initial indentation δ_0 of the sample was made under a controlled force F_0, given by Hertz model:

$$F_0 = \frac{3\,E\tan\theta}{4\,(1-\nu^2)}\delta_0^2 \qquad (1)$$

where E is the Young modulus, ν the Poisson ratio (usually assumed to be close to 0.5 for such gels [25]) and θ as defined above. It has been shown [26] that the effect of the tip curvature does not affect measurements as long as the penetration depth δ_0 is large, usually higher than 300 nm. Therefore δ_0 was chosen large enough (usually around 500 nm) allowing a sufficient contact area. In order to carry out microrheology measurements, a small perturbation $\delta(\omega)$ (frequency f from 1 Hz to 0.5 kHz, and $\omega = 2\pi f$ is the angular frequency) was superposed to the initial indentation. The perturbation being small, Eq. (1) can be linearized about the equilibrium. By the correspondence principle of LVE, in the ω–domain, one operates with complex quantities. Let δ^*, F^* be the complex indentation and force. Substracting the hydrodynamic drag $i\omega b(0)$ [16], the complex shear modulus $G^*(\omega)$ is given by:

$$G^*(\omega) = \frac{1-\nu}{3\,\delta_0\,\tan\theta}\Big\{\frac{F^*(\omega)}{\delta^*(\omega)} - i\omega b(0)\Big\} \qquad (2)$$

where $b(h)$ is a function accounting for the geometry of the tip and depends on the height h from tip to sample, and was measured [16] by extrapolation of the function at $h = 0$. Checking of the data was also carried out using other MLCT cantilevers on the same chip, and the same results were obtained (data not shown). Frequencies were varied from 1 Hz to 500 Hz, and signals corresponding to $\delta(\omega)$ and $F(\omega)$ were recorded, showing that 500 Hz is the upper frequency limit, beyond which spurious effects occur as we get close to the resonant frequency of the cantilever.

As it is possible that inhomogeneous structures appear within such polymer networks (depending on concentration and crosslinker), AFM experiments were repeated several times. At least 16 experiments per gel were made in the frequency range. Further indentation tests were also carried out to obtain the Young modulus (E) from Eq. (1). Histograms of E, G' and G'' (at 1 Hz) are shown (10% concentration gel) in Fig. 1. The data show that heterogeneities do not affect the rheological measurements so much, and confirms that $E \sim 3\,G'$ (at low frequencies), as expected for incompressible elastic materials ($\nu \sim 0.5$).
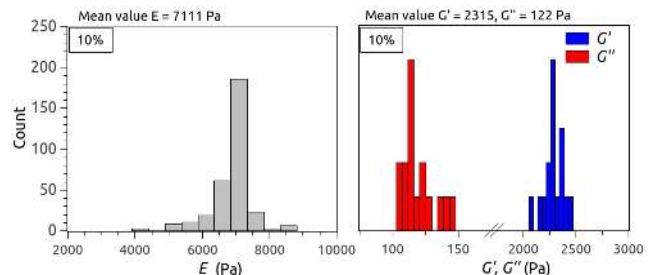

Fig. 1: Histograms showing the 10% gel rheological properties: elastic modulus (E) and dynamic moduli G' and G'' at 1 Hz. $E = 7111$ Pa ± 34 Pa, $G'(1Hz) = 2315$ Pa ± 25 Pa. Note that $E \sim 3\,G'$.

Rheometry measurements were carried out on a controlled stress rheometer (Malvern, Gemini 150) at low fre-

quencies [0.001 Hz − 2 Hz] in the linear regime (deformation of 1%), and possible slip was avoided. Interestingly, an excellent agreement was found between these measurements and AFM microrheology experiments for all gels, as seen in Fig. 2 where matching occurs around 2 Hz for the 10% gel. Note that with an adequate AFM equipment operating at lower frequencies, all data should be obtained only with the AFM. Still it is interesting here to use rheometry and match both sets of data.
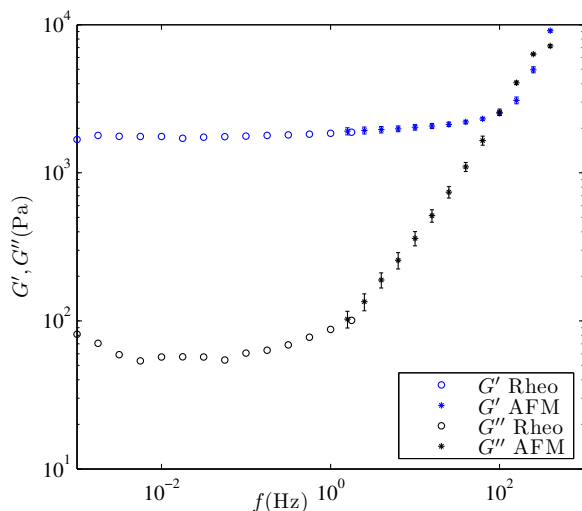

Fig. 2: Superposition of rheometrical (open circles) and AFM measurements (stars, with standard deviations shown). The acrylamide content is 10% in this case. $T = 25^{o}C$.

The variations of the dynamic moduli (Fig. 2) showed a constant elastic plateau modulus (G_N^0) at low frequencies ($G_N^0 \simeq 2300$ Pa). The gel underwent a glassy transition in the higher frequency regime as the AFM measurements did show. The slopes of both moduli G' and G'' vs. ω (slightly smaller than 1.0), were similar above 100 Hz.

Rheological modelling. To predict the observed behavior, a rheological model was used. The complex modulus $G^*(\omega)$ was related to a relaxation function $H(\lambda)$ using the formalism introduced by Winter and collaborators [2] :

$$G^*(\omega) = \int_0^\infty H(\lambda) \frac{i\omega\lambda}{1 + i\omega\lambda} \frac{d\lambda}{\lambda} \qquad (3)$$

$H(\lambda)$ is the continuous relaxation spectrum, the expression of which is shown in this work to model the LVE response from flow to glassy state. In particular, the flow regime was described by the function $H_f(\lambda)$, and associated complex modulus $G_f^*(\omega)$ from Eq. (3):

$$H_f(\lambda) = \begin{cases} n_f G_N^0 \left(\dfrac{\lambda}{\lambda_{max}} \right)^{n_f} & \text{if } \lambda \leq \lambda_{max} \\ \\ 0 & \text{if } \lambda > \lambda_{max} \end{cases} \qquad (4)$$

This power law behavior can describe the continuous relaxation time distribution required to model the plateau

regime observed for G' in Fig. 2 at low frequencies, while G'' decreases with slope $-n_f$. This model is unsuitable to describe the high frequency state, and consequently the BSW description [2] is insufficient to predict the data accurately. Therefore a fractional derivative model [3] was prefered and added to the previous one, to account for high frequency data. The corresponding expression for $G_g^*(\omega)$ in the transition, was simply given by :

$$G_g^*(\omega) = G_1 \frac{(i\omega\lambda_1)^b}{1 + (i\omega\lambda_1)^a} \qquad (5)$$

where a and b are the orders of fractional derivatives. Compatibility with thermodynamics [27] requires $0 < a \leq b$. This type of model accounts for the slopes in the glassy transition, as observed in the current data.

The coupling of the two linear models is insured by the simple relationship $G^*(\omega) = G_f^*(\omega) + G_g^*(\omega)$, and covers the whole frequency spectrum. The parameters of this global model are G_N^0, λ_{max}, n_f, a, b, G_1 and λ_1. Fig. 3 presents the role of each parameter, in a frequency range comparable with our experiments. G_N^0 appears naturally to be the classical elastic plateau modulus (Fig. 3). λ_{max} is the maximum relaxation time corresponding to the flow domain. In the case of gels, this specific time is out of reach since gels do not actually flow and exhibit a plateau even at very low frequencies [28]. $-n_f$ is the slope of G'' at low frequencies, in a log–log plot and is found to lie between -0.73 and -0.06. a represents the slopes of G' and G'' in the glass transition regime (with $a = b$ in Fig. 3). G_1 is the high frequency modulus of G', and is far above our data, so complementary rheological experiments would be necessary to reveal such high values of the limiting modulus [3]. λ_1 is a relaxation time related to the fine microstructure and is not shown in Fig. 3. Actually $1/\lambda_1$ is a typical crossover frequency between the glass and solid domains. Finally $b - a$ would correspond to the limiting slopes of G' and G'' moduli at the highest frequencies, not shown in Fig. 3. We found that $a = b$ leads to the optimal fit.

Fitting of the data was carried out for the four gels described above, characterized both in rheometry and AFM microrheology. The best-fitting values of the parameters were determined by minimizing a weighted sum of squared residuals. The weights were chosen from the data. Minimization was achieved using the Levenberg–Marquardt method. The initial guesses followed the discussion on the role of each single parameter (see Fig. 3).

The best-fitting values of the parameters are reported in Table 1 and the associated curves are presented in Figures 4–7. Very good agreement between the predictions and the model were obtained.

Discussion. – Let us look at the behavior of the plateau modulus G_N^0, which increases with c, the acrylamide concentration. G_N^0 is shown in log–log scale in Fig. 8. A power law dependence $G_N^0 \sim c^{3.0 \pm 0.3}$ is found from the data. This exponent can be compared to other values from the literature. Indeed, previous observations

Table 1: Best-fitting values of parameters used in the model for the different gels of concentrations 5%, 7.5%, 10% and 15%.

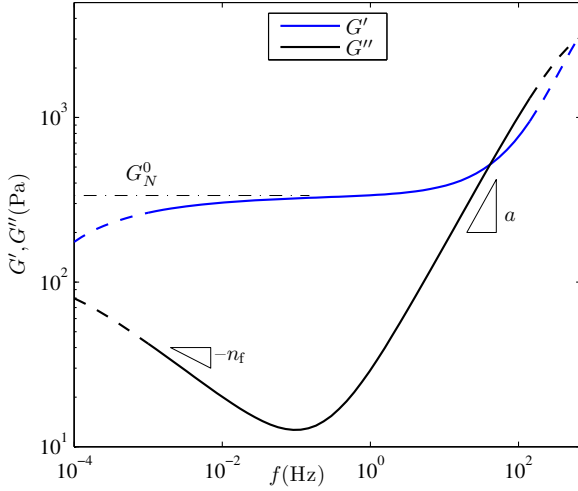| Gel	G_N^0(Pa)	$\lambda_{\max}$(s)	n_f	λ_1(s)	G_1(Pa)	$a = b$
5%	336	1.5×10^4	0.73	1.3×10^{-4}	1.0×10^4	0.82
7.5%	710	2.0×10^5	0.18	2.4×10^{-4}	1.0×10^4	0.85
10%	2307	9.0×10^9	0.08	2.4×10^{-4}	2.0×10^4	0.97
15%	8801	1.0×10^{10}	0.06	2.0×10^{-4}	5.9×10^4	0.98

Fig. 3: Significance of the model parameters: G_N^0 (plateau modulus), n_f (slope of G'' at low frequencies), and $a = b$ (slopes of G' and G'' at high frequencies). $\omega \sim 1/\lambda_{\max}$ corresponds to the intersection of G' and G'' occuring for very low frequencies (not shown). G_1 corresponds to a higher plateau modulus in G' for $\omega \sim 1/\lambda_1$, but is well above our data.
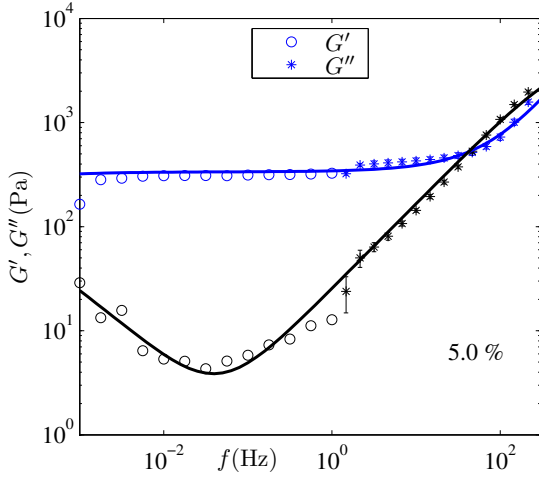

Fig. 4: Rheology of the 5% acrylamide gel. Rheometrical (open circles) and AFM (stars, with standard deviations shown) experimental data. Solid lines are the best model fits.
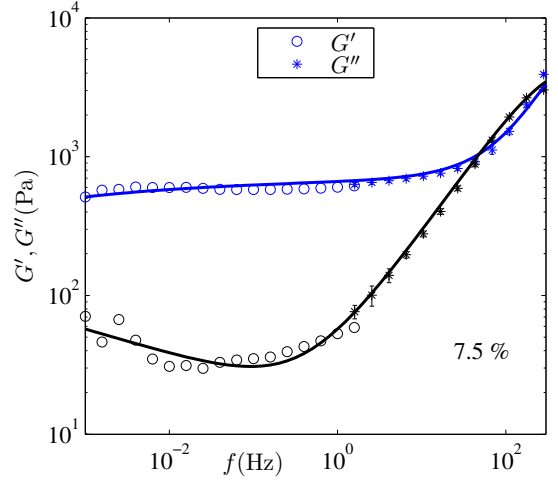

Fig. 5: Rheology of the 7.5% acrylamide gel. Rheometrical (open circles) and AFM (stars, with standard deviations shown) experimental data. Solid lines are the best model fits.
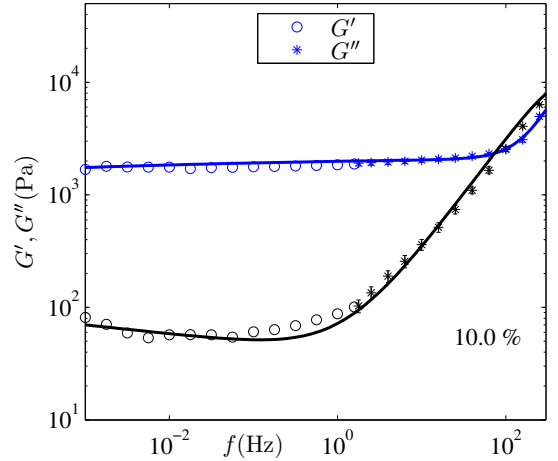

Fig. 6: Rheology of the 10% acrylamide gel. Rheometrical (open circles) and AFM (stars, with standard deviations shown) experimental data. Solid lines are the best model fits.

using combined light scattering and mechanical tests [22] report an exponent 2.55 using dynamic mechanical mea-

surements (or 2.35 using dynamic light scattering) as compared to the theory of de Gennes giving 2.25 for good solvents [23]. The exponent for G_N^0 is close to the exponent 2.55, found for collagen gels [29, 30] but larger than 1.4, obtained for entangled actin solutions [31].

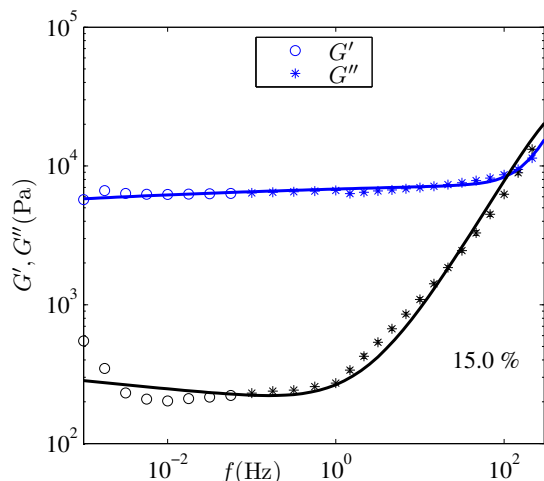The longest relaxation time $\lambda_{\max}$ does not seem to play

Fig. 7: Rheology of the 15% acrylamide gel. Rheometrical (open circles) and AFM (stars, with standard deviations shown) experimental data. Solid lines are the best model fits.
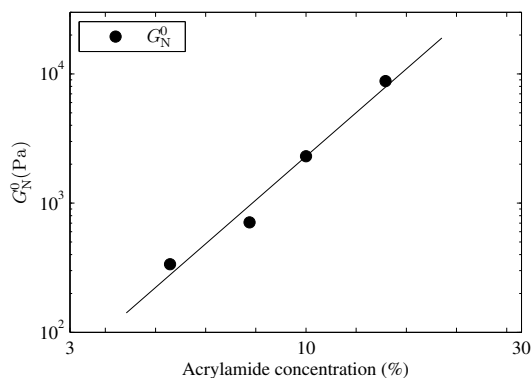

Fig. 8: Evolution of gel modulus G_N^0 vs. concentration. The slope of the power law exponent corresponds to 3.0 ± 0.3.

a significant role, as it is related to a possible crossover of the G' and G'' moduli at low frequencies which does not occur for such gels (in our frequency range) since they do not flow at low frequencies. However, $-n_f$, the low–frequency slope of G'' vs. ω, is a parameter of interest, and becomes closer to 0, as gel concentration increases. This emphasizes the fact that high concentration gels exhibit moduli with almost flat G' and G'' moduli (see gels in Figures 6–7 at 10% and 15% acrylamide concentration). Note that values of G' and G'' at low frequencies (0.001 Hz) using classical rheometry were difficult to obtain, due to the long experimental times required, therefore a larger uncertainty is unavoidable for n_f. Nevertheless, n_f increases as c decreases, meaning that a lower crosslinking could eventually lead to a crossing of G' and G'' at lower frequencies.

At higher frequencies, G' and G'' vs. f exhibit slopes a and b between 0.82 and 0.98 (see Table 1). In all cases, the optimum was found for $a = b$, and used in the optimisation method. Both G' and G'' exhibit a slope a, related to the fractional derivatives in the model. The dependence of

$G', G'' \sim \omega^{3/4}$ suggested in the litterature for semiflexible polymers [32] is therefore close to our data.

λ_1 was found to be almost constant $\sim 2.0 \times 10^{-4} s$, within experimental error, revealing no clear difference in the entanglement relaxational processes of the polyacrylamide gels at very high frequencies. Therefore, all four networks show similar trends at high frequencies.

Finally, the onset of the glass transition can be linked to the crossing of the G' and G'' moduli, at a typical frequency f_T. Above this crossing frequency, both moduli increase with a similar power dependence $G' \sim \omega^a$ and $G'' \sim \omega^a$, up to 500 Hz. This frequency is associated to a transition time $\lambda_T = 1/2\pi f_T$. As can be seen in Figures 4–7, when c increases, G' exhibits a longer plateau, and the crossing frequency f_T increases between 40 Hz and 190 Hz. It is therefore a signature of the gel. This frequency f_T can be found by inspection of G'. On the plateau, $G' \sim G_N^0$, then for higher frequencies, using Eq.(5) and $a = b$, we find $G' \sim G_1 \cos(\pi a/2)(\omega\lambda_1)^a$ since $\omega\lambda_1 << 1$ in this domain. Therefore the transition frequency f_T reads:

$$f_T = \frac{1}{2\pi\lambda_1} \left(\frac{G_N^0}{G_1 \cos(\pi a/2)} \right)^{1/a} \qquad (6)$$

The increase of f_T with c is confirmed by inspection of Table 1. $\frac{G_N^0}{G_1}$ increases with c, since G_N^0 varies faster than G_1 with c, while $\cos(\pi a/2)$ decreases, thus the ratio $\frac{G_N^0}{G_1 \cos(\pi a/2)}$ increases and $1/a$ increases with c as well. Since λ_1 is almost constant, we deduce that f_T increases with polymer concentration. f_T can be understood as an important parameter characterizing the transition from a polymer gel to a system where single–chains may fluctuate between crosslinks. In this respect, it has been shown that polymeric systems undergo transitions, in the context of the Rouse model [23] or considering hydrodynamic interactions [24]. Theses processes involve a correlation length ξ, i.e. a characteristic length scale which estimates the fluctuations and is usually measured by elastic and light scattering measurements. The correlation length ξ usually varies like $\xi \sim c^{-0.75}$ [23], as verified experimentally for polyacrylamide gels [33]. The theoretical frequency f_T possibly varies as $f_T \sim c^{2.75}$ [23] or $c^{2.25}$ [24] for entangled polymeric networks. In the context of gels, these features may show differences and have not yet been tested. Our measurements provide accurate data on the crossing of G' and G'', thanks to AFM measurements. As the bisacrylamide concentration is small, one can except the correlation length to be rather constant, on the order or 10nm as shown previously [34], thus ξ and f_T will depend mainly on polymer concentration c. A careful analysis of the data in Fig. 9 shows a power behavior $f_T \sim c^{1.6\pm0.1}$. This exponent is slightly below the exponent predicted previously [24]. Nevertheless, the change in f_T was captured, as an important network parameter – sensitive to concentration c – accessible from such measurements. Thus, our AFM–technique, coupled with classical rheology, brings together important information on the dynamics of such gels.
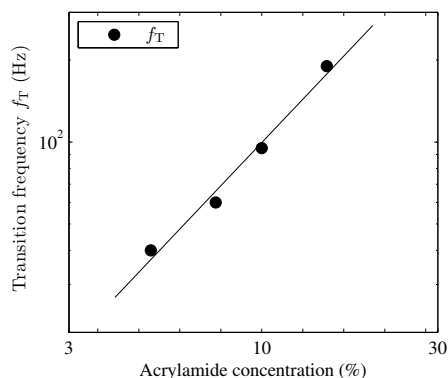
Fig. 9: Evolution of transition frequency f_T vs. concentration. The power law exponent is 1.6 ± 0.1.

Conclusions. – In this paper, we showed the ability of the AFM–based microrheology technique to extend classical rheological properties of gels. Both methods were used and matched on the elastic plateau, with higher frequency data obtained thanks to the AFM technique.

A model was proposed to predict the experimental data. It includes a multiple relaxation spectrum at low frequencies combined with a fractional model for higher frequencies. The model parameters are related to the gels physical properties. In particular, a new characteristic frequency f_T has been introduced at the onset of the glass transition and was compared to previous theories.

Further applications of the model may be considered with other physical (or chemical) gels, as well as the study of biological systems, such as actin, tubulin newtworks, and finally living cells [16]. Indeed, this model, coupled with the use of high frequency AFM measurements, may allow to investigate more complex materials and provide simple parameters to distinguish them.

REFERENCES

[1] Larson R., *The Structure and Rheology of Complex Fluids* (Oxford University Press, New York) 1999.
[2] Baumgaertel M., Rosa M. E. D., Machado J., Masse M. and Winter H. H., *Rheol. Acta* , **31** (1992) 75.
[3] Palade L. I., Verney V. and Attané P., *Rheol. Acta* , **35** (1996) 265.
[4] Gittes F., Schnurr B., Olmsted P. D., MacKintosh F. C. and Schmidt C. F., *Phys. Rev. Lett.* , **79** (1997) 3286.
[5] Dasgupta B. R. and Weitz D. A., *Phys. Rev. E* , **71** (2005) 021504.
[6] Verdier C., Longin P. Y. and Piau M., *Rheol. Acta* , **37** (1998) 234.
[7] Longin P. Y., Verdier C. and Piau M., *J. Non-Newt. Fluid Mech.* , **76** (1998) 213.
[8] Sollich P., Lequeux F., Hébraud P. and Cates M. E., *Phys. Rev. Lett.* , **78** (1997) 2020.
[9] Sollich P., *Phys. Rev. E* , **58** (1998) 738.
[10] Fabry B., Maksym G. N., Butler J. P., Glogauer M., Navajas D. and Fredberg J. J., *Phys. Rev. Lett.* , **87** (2001) 148102.
[11] Mason T. G., Ganesan K., van Zanten J. H., Wirtz D. and Kuo S. C., *Phys. Rev. Lett.* , **79** (1997) 3282.
[12] Crocker J. C., Valentine M. T., Weeks E. R., Gisler T., Kaplan P. D., Yodh A. G. and Weitz D. A., *Phys. Rev. Lett.* , **85** (2000) 888.
[13] Chaudhuri O., Parekh S. H. and Fletcher D. A., *Nature* , **445** (2007) 295.
[14] Dalhaimer P., Discher D. E. and Lubensky T. C., *Nat. Physics* , **3** (2007) 354.
[15] McGuiggan P. and Yarusso D., *J. Mat. Research* , **19** (2004) 387.
[16] Alcaraz J., Buscemi L., Grabulosa M., Trepat X., Fabry B., Farr R. and Navajas D., *Biophys. J.* , **84** (2003) 2071.
[17] Hiratsuka S., Mizutani Y., Tsuchiya M., Kawahara K., Tokumoto H. and Okajima T., *Ultramicroscopy* , **109** (2009) 937.
[18] Abidine Y., Laurent V. M., Michel R., Duperray A. and Verdier C., *Comput. Methods Biomech. Biomed. Eng* , **16** (2013) 15.
[19] Radmacher M., Tillmann R. W. and Gaub H. E., *Biophys. J.* , **64** (1993) 735.
[20] Pelham R. J. and Wang Y., *Mol. Biol. Cell* , **10** (1999) 935.
[21] Ambrosi D., Duperray A., Peschetola V. and Verdier C., *J. Math. Biol.* , **58** (2009) 163.
[22] Hecht A.-M. and Geissler E., *J. Physique* , **39** (1978) 631.
[23] de Gennes P.-G., *Macromolecules* , **9** (1976) 587.
[24] de Gennes P.-G., *Macromolecules* , **9** (1976) 594.
[25] Boudou T., Ohayon J., Picart C. and Tracqui P., *Biorheology* , **43** (2006) 721.
[26] Rico F., Roca-Cusachs P., Gavara N., Farr R., Rotger M. and Navajas D., *Phys. Rev. E* , **72** (2005) 021914.
[27] Bagley R. L. and Torvik P. J., *J. Rheol.* , **27** (1983) 201.
[28] Verdier C., Etienne J., Duperray A. and Preziosi L., *C. R. Acad. Sci. Phys.* , **10** (2009) 790.
[29] Iordan A., Duperray A., Gérard A., Grichine A. and Verdier C., *Biorheology* , **47** (2010) 277.
[30] Vader D., Kabla A., Weitz D. and Mahadevan L., *PLoS One* , **4** (2009) e5902.
[31] Hinner B., Tempel M., Sackmann E., Kroy K. and Frey E., *Phys. Rev. Lett.* , **81** (1998) 2614.
[32] Gittes F. and MacKintosh F. C., *Phys. Rev. E* , **58** (1998) R1241.
[33] Wu C., Quesada M. A., Schneider D. K., Farinato R., Studier F. W. and Chu B., *Electrophoresis* , **17** (1996) 1103.
[34] Orakdogen N. and Okay O., *Polymer Bulletin* , **57** (2006) 631.